# Shock Waves produced by Impulsive Load: Equation of State Effects

S. A. Lifits
Landau Institute for Theoretical Physics, Moscow

S. I. Anisimov*
Ecole Polytechnique, Centre de Physique Theorique, Palaiseau

J. Meyer-ter-Vehn
Max-Planck-Institut für Quantenoptik, Garching

Z. Naturforsch. **47a**, 453–459 (1992); received September 9, 1991

A numerical study of the flow after impulsive load of a plane material surface is carried out. It is shown that the flow is asymptotically self-similar provided one can neglect the cold components in the equation of state. In this case the effective exponent $s(t) = \mathrm{d}\ln(X_s)/\mathrm{d}\ln(t)$, derived from the shock trajectory $X_s(t)$ does not depend on the initial pressure pulse and approaches the exponent $\alpha$ of the self-similar problem for time $t \to \infty$. For equations of state containing a cold pressure term, $s(t)$ is larger than $\alpha$ and changes non-monotonically with time. Some features of the flow related to the presence of cold components in pressure and internal energy are discussed.

*Key words:* Shock wave, Impulsive load, Equation-of-state, High pressure, Self-similar flow.

## 1. Introduction

In studies of the thermodynamic properties of matter at very high pressures dynamic methods are most important. These methods employ strong shock waves generated by high explosives, hypervelocity impact, laser or particle beams. "Classical" dynamic methods worked out for high-explosive experiments are based on the compression of a material by steady state plane shock waves. Measuring two shock parameters (e.g. shock velocity and pressure, or shock velocity and mass velocity) and using the conservation laws one can obtain the Hugoniot curve of a material. This approach provided extensive information on the equation of state (EOS) and transport properties of many materials in the pressure range up to $\approx 5$ Mbar [1]. For higher pressures, high power lasers and high-current particle beams can be employed. In this case, however, some problems arise connected with preheating of unshocked matter by fast electrons and X-rays. To avoid preheat effects one should use sufficiently thick targets. Of course, this implies a sharp increase of laser energy for increasing pressure. According to [2], the laser energy needed for an EOS-experiment at pressure $p$ scales like $E_{las} \sim p^6$. This considerably restricts the potential of the "classical" scheme based on steady-state shock waves. Non-stationary flows with strong shock waves can also be employed in EOS-studies. However, this approach demands, generally, rather complicated computer calculations. A simpler situation occurs when a non-stationary flow is self-similar. For such flows, the shock wave propagates according to the law $X_s = A t^{\alpha}$, where $\alpha$ is a similarity exponent. In [3], a similarity solution was obtained describing the flow generated by an impulsive load, and the dependence of the similarity exponent upon EOS parameters was found. Unfortunately, one can expect a self similar flow only for a certain class of the equations of state [4, 5]. The corresponding condition reads

$$(\partial p/\partial V)_s = p \cdot F(V), \tag{1}$$

where the partial derivative is calculated at constant entropy and $F(V)$ is an arbitrary function of volume. The EOS considered in [3] was taken in the form

$$p(V,E) = (E/V) \cdot \Gamma(V), \tag{2}$$

where $E$ is the specific energy and $\Gamma(V)$ is the Grüneisen coefficient. EOS (2) satisfies condition (1), but it includes only the thermal component of the pressure.

* On leave from Landau Inst. Theor. Phys., Moscow.
Reprint requests to Dr. J. Meyer-ter-Vehn, Max-Planck-Institut für Quantenoptik, D-8046 Garching.

0932-0784 / 92 / 0300-0453 $ 01.30/0. – Please order a reprint rather than making your own copy.

A more realistic EOS of condensed matter must also include the cold pressure term $p_c(V)$ which describes the elastic properties of matter at zero temperature. According to [4, 5], the simplest EOS which agrees resonably with experimental data can be written in the form

$$p(V,E) = p_c(V) + \Gamma(V,E)/V \cdot [E - E_c(V)], \quad (3)$$

where

$$p_c = -\partial E_c/\partial V,$$

and $E_c(V)$ is the internal energy at zero temperature. Equation (3) does not satisfy condition (1). Thus, strictly speaking, no self-similar motion is expected for condensed matter. However, one observes that EOS (3) approaches EOS (2) at extremely high shock pressures when the thermal components of pressure and internal energy are much greater than the cold ones. In order to find out the conditions at which the similarity approach [3] provides a reasonably good description of condensed matter motion generated by impulsive load, an exact numerical solution of the gasdynamic equations was obtained in [6]. Two different versions of EOS were used: i) a semi-empirical EOS of the SESAME library [7] and ii) an EOS in the form (3) with $p_c$ and $E_c$ taken from paper [8] and $\Gamma(V)$ taken from paper [3]. In both cases it was found that the time dependence of the shock trajectory can be approximated by the similarity-type formula $X_s = Bt^s$, but with the exponent s considerably larger than the similarity exponent $\alpha$ obtained in [3]. Moreover, the exponent s appeared to be larger than the upper limit for the similarity exponent $\alpha$ obtained in [4].

## 2. The Model

In the present paper, a more detailed numerical study of the impulsive load problem is carried out. We study both "selfsimilar" and "non-selfsimilar" equations of state and find the interval of changes of the effective exponent s determined by

$$s = \mathrm{d}(\ln X)/\mathrm{d}(\ln t). \quad (4)$$

First we investigate the transient process leading to the formation of the similarity flow (in cases when similarity motion can be reached). This seems to be important since in [3] neither the spectrum of the similarity exponent $\alpha$ nor the stability of the self-similar solution were studied. Finally, we calculate the spatial structure generated by impulsive load and find some features related to the presence of cold components in the pressure and the internal energy.

The problem under consideration can be formulated in the following way. The pressure pulse with amplitude $p_0$ is applied during the time $\tau$ to the boundary at $x = 0$ of the half-space $x > 0$ filled with matter and having $p = p(V,E)$ as EOS. The flow is to be determined at times $t \gg \tau$. To solve the problem, a numerical method based on the fully conservative 1D Lagrangean scheme is applied. Three different EOS's are considered (they will be referred to as I, II and III): I – the Mie-Grüneisen type equation (2) without a cold pressure term; II – the EOS of form (3) used earlier in [4]; III – a more complex single-phase semiempirical EOS of form (3) with the Grüneisen coefficient $\Gamma(E)$ depending on the energy $E$. The values of the parameters in all three EOS's have been chosen to fit aluminium metal at high pressures. We discuss the results obtained with each of the EOS's separately.

## 3. Discussion of Results

### *3a) EOS I*

The most important problem in the case of EOS I is the formation of self-similar flow from the initial state. Since this state differs in general from the self-similar solution for $t \to 0$, the numerical calculation provides certain information on the stability of the similarity solution. Calculations were carried out for the EOS I defined in (2) with the Grüneisen coefficient given by the relation

$$\Gamma(V) = 2/3 + (\Gamma_0 - 2/3) \cdot (Z_0^2 + 1)/(Z_0^2 + Z^2), \quad (5)$$

where $Z = V_0/V$ with the specific volume $V_0 = 1/\varrho_0$ at normal density $\varrho_0$ and constants $\Gamma_0$ and $Z_0$. Approximation (5) has been proposed by Bushman [9] and was used in [3]. In the calculations, amplitude, duration and temporal profile of the initial pressure pulse were varied. Different values of the parameters $\Gamma_0$ and $Z_0$ were considered including those studied earlier in [3].

It follows from the calculations that in all runs with EOS I a limiting similarity solution is reached independently of the parameters of the initial pressure pulse. The transient time appeared to be about one order of magnitude longer than the pressure pulse duration. In Fig. 1 the shock front trajectory is plotted in a $\ln x$, $\ln t$ plane. The trajectory is almost linear. However, a more detailed analysis shows that the ef-

Table 1. Comparison of time evolution exponents $\alpha$ for pure selfsimilar flow (taken from [3]) and $s(t=\infty)$ obtained from (4) using numerical simulation; $\Gamma_0$ and $Z_0$ are parameters of EOS I (3).

| $\Gamma_0$ | $Z_0$ | $\alpha$ | $s(t=\infty)$ |
|---|---|---|---|
| | 0.50 | 0.6304 | 0.6310 |
| 1.78 | 0.65 | 0.6288 | 0.6298 |
| | 0.80 | 0.6273 | 0.6280 |
| | 0.50 | 0.6321 | 0.6330 |
| 2.02 | 0.65 | 0.6305 | 0.6313 |
| | 0.80 | 0.6289 | 0.6297 |
| | 0.50 | 0.6331 | 0.6340 |
| 2.19 | 0.65 | 0.6312 | 0.6322 |
| | 0.80 | 0.6311 | 0.6310 |

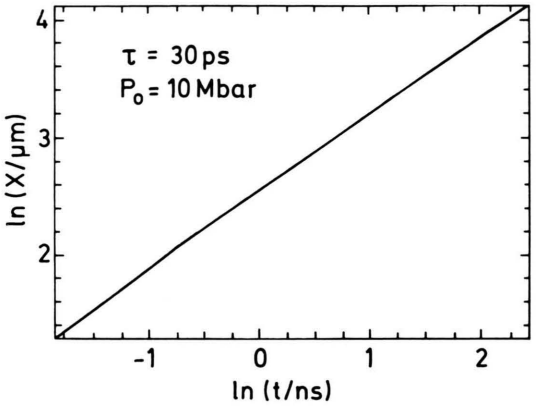


Fig. 1. Shock trajectory for EOS I with $\Gamma_0 = 2.19$ and $Z_0 = 0.65$; box-shaped initial pressure pulse of 30 ps duration and 10 Mbar amplitude.

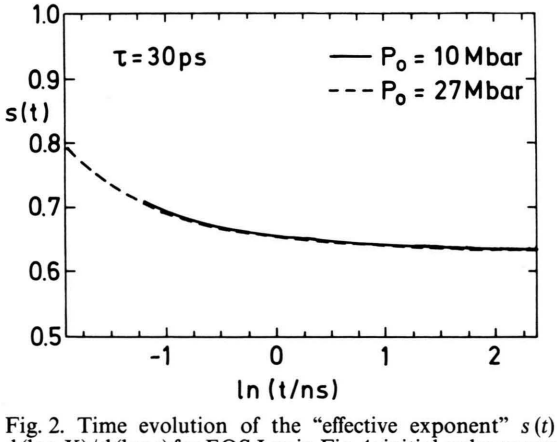


Fig. 2. Time evolution of the "effective exponent" $s(t) = \mathrm{d}(\log X)/\mathrm{d}(\log t)$ for EOS I as in Fig. 1; initial pulse parameters: duration 30 ps, amplitude 27 Mbar (solid line) and 10 Mbar (broken line).

fective exponent $s$, given by (4), changes slowly with time (see Figure 2). The limiting value of $s$ at sufficiently large $t$ approaches the similarity exponent $\alpha$ determined by expression (3) monotonically. In Table 1, limiting values of $s$ are compared with values of $\alpha$, determined in [3].

One can see that differences between $s$ at $t=\infty$ and $\alpha$ do not exceed 0.001 in all cases considered. Moreover, all the values of $s$ for $t\to\infty$ are larger than the corresponding values of $\alpha$; this can be explained simply by the fact that time was limited in the calculation. It is interesting to note that the transient behavior of $s(t)$ does not depend on the amplitude of the initial pressure pulse (see Figure 2).

Spatial profiles of velocity, specific volume and pressure obtained from the numerical solution at time $t=11.81$ nsec ($\tau=30$ psec, $P_0=10$ Mbar) are shown in Figs. 3 to 5. They coincide exactly with the corresponding profiles obtained in [3]. Thus, for EOS I and different initial pressure pulses the limiting similarity solution is reached at times $t\gg\tau$.

### *3b) EOS II*

In the case of EOS II, cold components of the pressure and the internal energy are taken into account. As in [6], this is done by using the results of [8], but the present analysis goes far beyond [6] by studying the numerical solution in much finer detail and clarifying its relation to the selfsimilar case. The EOS II is written in the form

$$\begin{aligned} P(V,E) &= p_c(V) + \Gamma(V)\cdot[E-E_c(V)]/V, \\ E_c &= E_0\exp(-a)\cdot(1+a+0.05\,a^3), \\ P_c &= -\partial E_c/\partial V, \quad a=\eta[(V/V_0)^{1/3}-1] \end{aligned} \tag{6}$$

with constants $E_0 = 1.193\times10^4$ J/g and $\eta = 4.71$. For the Grüneisen coefficient, approximation (5) is used with $\Gamma_0 = 2.19$ and $Z_0 = 0.65$ (see [3]). It is easy to see that the EOS II (6) does not satisfy condition (1). However, at very large shock pressures when the second term in (6) is much greater than the first one, one can expect that the similarity solution will provide a good approximation. In Fig. 6, the density ratio across the shock front $\sigma = \varrho_s/\varrho_0 = V_0/V_s$ and the ratio $(E_c/E)_s$ of the cold energy component $E_c$ to the total energy $E$ are presented as functions of the shock pressure $p_s$. Here the index s refers to values just behind the shock front. The initial state is chosen to be $p_0 = 0$, $\varrho_0 = 2.7$ g/cm$^3$. From the energy curve it can be con-

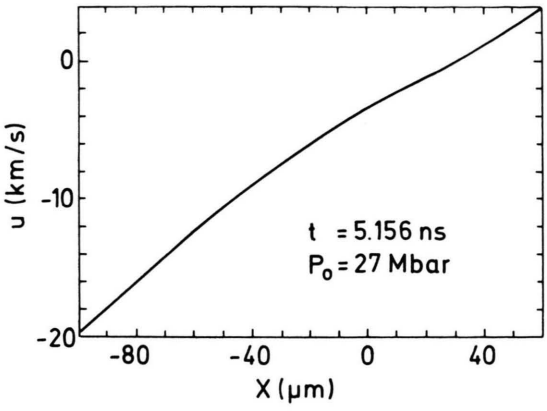


Fig. 3. Spatial velocity profile at $t = 5.156$ ns for EOS I; initial pulse parameters: duration 30 ps, amplitude 27 Mbar.

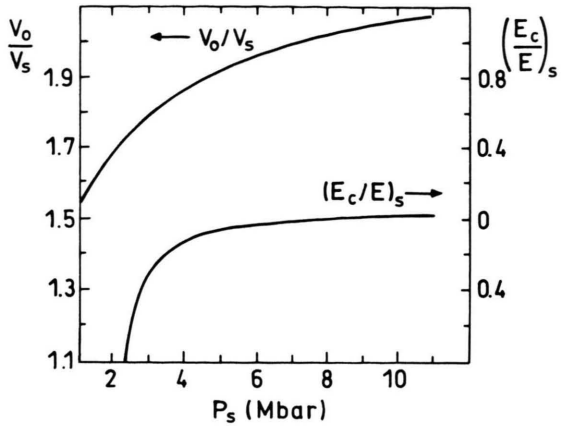


Fig. 6. Density jump across the shock front, $\varrho_s/\varrho_0 = V_0/V_s$, and the ratio $(E_c/E)_s$ of the cold energy component to the total energy behind the shock front as functions of shock pressure $p_s$ for EOS II.

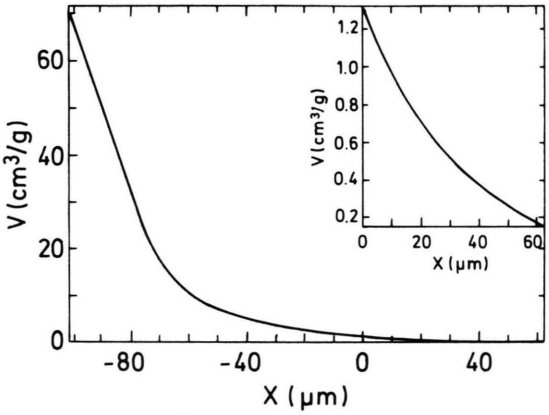


Fig. 4. Spatial profile of specific volume $V = 1/\varrho$; parameters as in Figure 3.

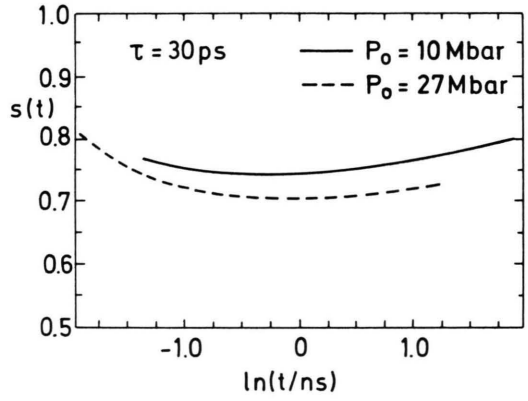


Fig. 7. Time evolution of the "effective exponent" $s(t)$; same as Fig. 2, but for EOS II.

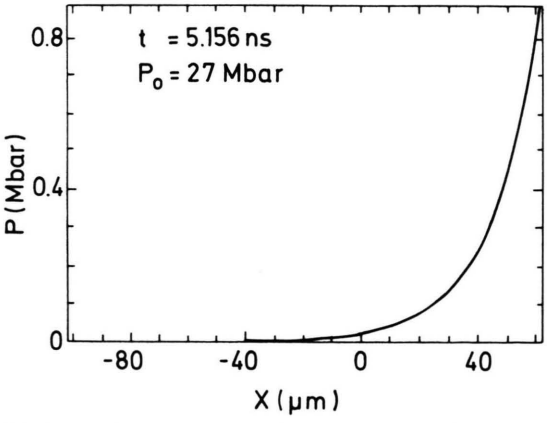


Fig. 5. Spatial pressure profile; parameters as in Figure 3.

cluded that, at shock pressures $p_s > 5$ Mbar, where $(E_c/E)_s$ vanishes, EOS I can be considered to be a good approximation, at least for the Hugoniot calculation. This does not mean that EOS I also gives a good description of the whole flow structure.

Now we discuss the numerical solution of the problem with EOS II. In Fig. 7, the time dependence of the "effective exponent" s, defined by (4), is presented for two different amplitudes of the initial pressure pulse, $p_0 = 10$ Mbar and 27 Mbar. In contrast to the case of EOS I the function $s(t)$ is now non-monotonic. At initial times, $s(t)$ decreases reflecting the formation of some regular flow regime. In the case of EOS I such a regime would correspond to the similarity flow. In the

case of EOS II, $s(t)$ reaches a minimum and then starts to grow slowly for larger times. The minimum values of $s$ depends on the initial pressure amplitude. It decreases for increasing $p_0$, but always remains larger than the similarity exponent obtained for the same EOS parameters but without cold components of pressure and internal energy.

The growth of $s(t)$ at large times is connected with the damping of the shock wave. In the limiting case $t \to \infty$ (at shock pressures $p_s \leqq 100$ kbar), the shock wave is transformed into an acoustic wave propagating at constant speed $c_s$. This case would correspond to the limiting value of the similarity exponent $s = 1$. Note that in the case of EOS II (in contrast to EOS I) the transient behavior of $s(t)$ depends on the amplitude of the initial pressure pulse (see Figure 7).

In Figs. 8 and 9, spatial profiles of velocity and specific volume are shown at time $t = 7.66$ ns ($p_0 =$ 10 Mbar, $\Gamma_0 = 2.19$, $Z_0 = 0.65$). The comparison of Figs. 3 and 4 with Figs. 8 and 9 shows that the profiles obtained with EOS I are very different from those obtained with EOS II. The most characteristic feature appearing in the latter case is the second shock front moving in the same direction as the principal one. This shock wave is clearly seen in Fig. 9 at $x \approx 10$ μm with a density jump from 1.92 to 2.33 g/cm$^3$. The jump of flow parameters across the shock can be shown to satisfy the Hugoniot relation. Spontaneous creation of the shock in a region of expanding flow can be explained as the result of an interplay between the two components of the total pressure. The density decrease due to adiabatic expansion of the shock-compressed material leads to a fast drop of the cold pressure component; the thermal pressure component decreases more slowly. At densities below solid density, the cold pressure component is negative. Being considered as a function of coordinate $x$, the cold pressure reaches its minimum at a certain point and then increases slowly reaching the zero value at the vacuum front where the density goes to zero. In the vicinity of the cold pressure minimum the gradient of the total pressure initially directed towards the principal shock front can, under certain conditions, change its sign, which leads to the generation of the second shock. Note that this anomalous behavior takes place in the region of the phase diagram corresponding to the liquid-gas phase transition. The EOS II has a very low accuracy in this region.

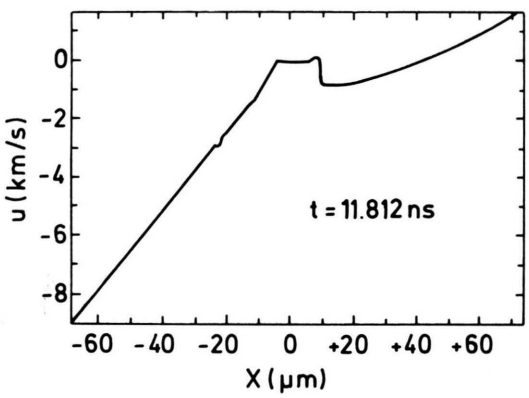


Fig. 8. Spatial velocity profile at $t = 11.812$ ns for EOS II; initial pulse parameters: duration 30 ps, amplitude 10 Mbar. A second shock front appears at $x \approx 10$ μm.

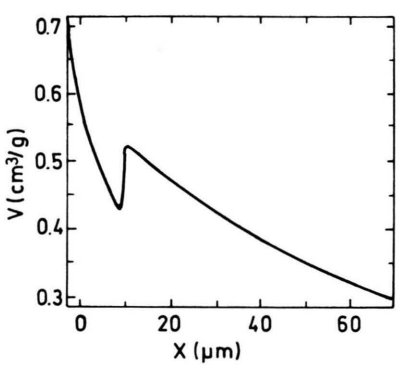


Fig. 9. Spatial profile of specific volume for EOS II; parameters as in Figure 8.

### *3c) EOS III*

A more accurate analysis in the framework of a single-phase EOS can be carried out using the EOS III proposed by Bushman and Fortov [5, 7]. This EOS can be written in form (3) with

$$E_c(V) = B_0 V_0/(m-n) \cdot (Z^m/m - Z^n/n) + E_s,$$
$$\Gamma(V,E) = (\Gamma(V) - \Gamma_i)/(1 + Z^{-2/3}[E - E_c(V)]/E_a), \quad (7)$$

where $\Gamma(V)$ is given by (5), $E_s$ is the energy of sublimation, and $E_a$, $B_0$, $m$, $n$ are constants. The values of the constants were calculated by Bushman [7] (see also [10]). EOS III given by the combination of (3) and (7) has the correct asymtotic behavior in the limits of high and low densities and well describes shock wave experiments in the intermediate region [7].

Calculations with EOS III were carried out in the same range of parameters as with EOS I and EOS II. The "effective exponent" $s(t)$ obtained from these cal-

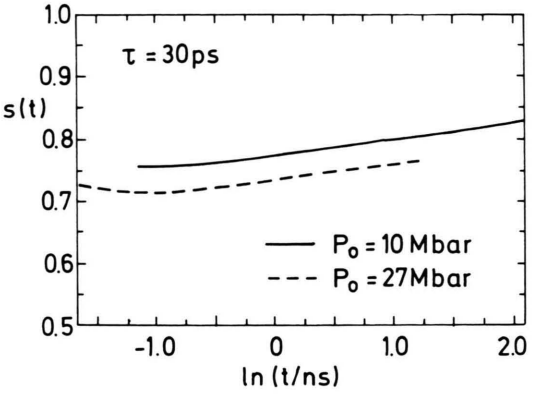


Fig. 10. Time evolution of the "effective exponent" $s(t)$; same as Fig. 2, but for EOS III.

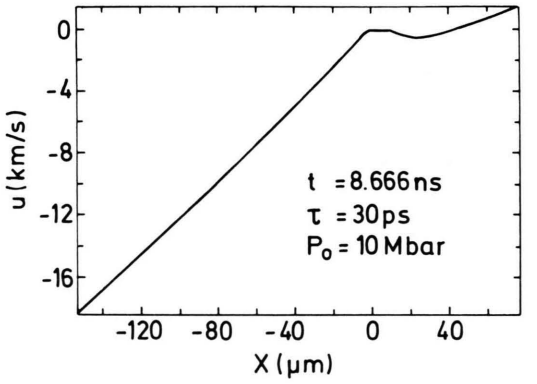


Fig. 11. Spatial velocity profile at $t = 8.666$ ns for EOS III; parameters as in Figure 8. No second shock front appears.

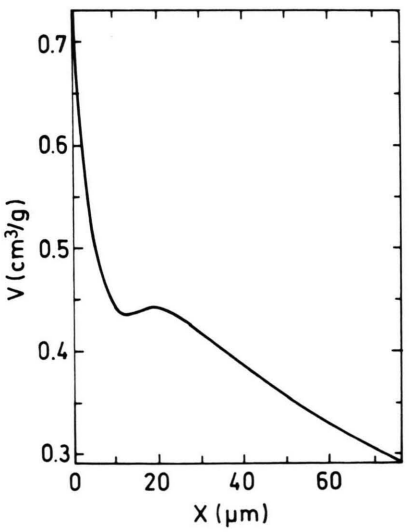


Fig. 12. Spatial profile of specific volume for EOS III; parameters as in Figure 8.

culations is shown in Figure 10. The two curves correspond to initial pressure amplitudes of 10 and 27 Mbar and a pulse duration of $\tau = 30$ psec. The qualitative behavior of $s(t)$ looks similar to that obtained for EOS II, but the numerical values of $s$ are different. We conclude therefore that the law of shock wave propagation is rather sensitive to the particular from of the EOS, and the measurement of shock velocities can provide useful information concerning the EOS. The spatial profiles of velocity and specific volume at the time $t = 8.666$ ns are drawn in Figs. 11 and 12. The profiles are qualitatively similar to those shown in Figs. 8 and 9, obtained for EOS II. The trend for the formation of the second shock is observed in the region between 10 and 20 μm at a density of about 2.3 g/cm$^3$, which is below the normal density of aluminium. This is the region where the minimum of the cold pressure is reached and the single-phase state of the material becomes thermodynamically unstable.

## Conclusion

The numerical calculations show that for EOS I self-similar flow is reached asymptotically at times $t \gg \tau$. The similarity exponent for this flow agrees well with that obtained in [3] as an eigenvalue of the set of ordinary differential equations. It is also found that the "relaxation time" which is needed to reach the self-similar regime of shock wave propagation does not depend on the amplitude of the initial pressure pulse in this case. Using EOS II and EOS III, similarity flow is not established. The effective similarity exponent $s = \mathrm{d}(\ln X)/\mathrm{d}(\ln t)$ changes slowly with time and is larger than that in the absence of the cold part of the pressure. We emphasize that special care is needed to obtain information on the time dependence of $s$ from the numerical solution.

The flow structure obtained with EOS II and EOS III is more complicated than the structure in case of EOS I. We observe, in particular, the instability of single phase expansion flow in the region where the cold pressure component has a minimum. The effect of this instability on the flow structure depends on the particular from the EOS. It is clear that a more sophisticated, multiphase EOS has to be used to describe more correctly the expansion flow in this region of parameters. Note, however, that an additional problem of phase transition kinetics arises when the flow is described as a multiphase one.

A flow of the type considered above can be easily produced in laser-matter interaction experiments. An experimental study of the flow structure (e.g. a check of shock formation in the expansion flow) would provide a sensitive method to examine the applicability of different semi-empirical EOS's in the vicinity of the two-phase region of the phase diagram.

*Acknowledgements*

This work was supported in part by the Bundesministerium für Forschung und Technologie and Euratom. Part of this work was done at the Centre de Physique Theorique of the Ecole Polytechnique at Palaiseau; one of the authors (S.A.) thanks Prof. G. Laval for his hospitality and helpful discussions and CNRS for support as a visiting professor. The authors thank Dr. A. Bushman for important advice concerning the equations of state used in this paper.

[1] L. V. Altshuler, Uspekhi Fiz. Nauk **85,** 197 (1965).
[2] S. I. Anisimov, A. M. Prokhorov, and V. E. Fortov, Uspekhi Fiz. Nauk **142,** 3, 395 (1984).
[3] S. I. Anisimov and V. A. Kravchenko, Z. Naturforsch. **40a,** 8 (1984).
[4] Ya. B. Zeldovich and Yu. P. Raiser, Physics of Shock Waves and High-Temperature Hydrodynamic Phenomena, Academic Press, New York 1966.
[5] A. V. Bushman and V. E. Fortov, Usp. Fiz. Nauk **140,** 177 (1983) [Sov. Phys. Usp. **26,** 465 (1983)].
[6] J. Meyer-ter-Vehn and R. Schmalz, Z. Naturforsch. **42a,** 1096 (1987).
[7] A. V. Bushman, private communication.
[8] SESAME '83: Report on the Los Alamos Equation-of-state Library. T4-Group, Los Alamos National Laboratory Report LALP-83-4, Los Alamos, New Mexico 1983.
[9] J. M. Rose and R. J. Smith, Phys. Rev. **29,** 2963 (1984).
[10] A. V. Bushman, A. L. Ni, and V. E. Fortov, in: Uravnenie sostoyaniya v ekstremalnykh usloviyakh (Equation Of State Under Extreme Conditions), ITPM SO AN SSSR (Inst. Theor. & Appl. Mech., Sibirian Branch of USSR Acad. Sci.), Novosibirsk 1981, p. 3.